Submitted to Nuclear Instruments and Methods

UCRL-20143
Preprint

RECEIVED
LAWRENCE
RADIATION LABORATORY

LIBRARY AND
DOCUMENTS SECTION

BETATRON AMPLITUDE GROWTH UPON TRAVERSING RESONANCES DURING THE COMPRESSION CYCLE OF AN ELECTRON RING ACCELERATOR

L. J. Laslett and W. A. Perkins

May 21, 1971

AEC Contract No. W-7405-eng-48

TWO-WEEK LOAN COPY

This is a Library Circulating Copy which may be borrowed for two weeks. For a personal retention copy, call Tech. Info. Division, Ext. 5545

UCRL-20143 c.2

28

DISCLAIMER

This document was prepared as an account of work sponsored by the United States Government. While this document is believed to contain correct information, neither the United States Government nor any agency thereof, nor the Regents of the University of California, nor any of their employees, makes any warranty, express or implied, or assumes any legal responsibility for the accuracy, completeness, or usefulness of any information, apparatus, product, or process disclosed, or represents that its use would not infringe privately owned rights. Reference herein to any specific commercial product, process, or service by its trade name, trademark, manufacturer, or otherwise, does not necessarily constitute or imply its endorsement, recommendation, or favoring by the United States Government or any agency thereof, or the Regents of the University of California. The views and opinions of authors expressed herein do not necessarily state or reflect those of the United States Government or any agency thereof or the Regents of the University of California.

Submitted to
Nuclear Instruments and Methods

UCRL-20143
ERAN-118

BETATRON AMPLITUDE GROWTH UPON TRAVERSING RESONANCES DURING THE COMPRESSION CYCLE OF AN ELECTRON RING ACCELERATOR†

L. J. Laslett and W. A. Perkins

Lawrence Radiation Laboratory
University of California
Berkeley, California

May 21, 1971

Abstract

In an electron ring accelerator electrons are often injected into a magnetic field with index $n = -(r/B_z)(dB_z/dr)$ of about 0.5. For extraction and axial acceleration of the ring, n must approach zero and several betatron resonances are crossed. Following particles on a computer through simulated fields (which approximate measured experimental fields) has elucidated which resonances are important and which magnetic field perturbations cause large growth for a particular geometry and coil-energizing sequence. Analytical formulas for resonance growth also have been derived and checked against the computer calculations. These equations indicate the important driving terms of the field and are convenient for estimating the expected growth on traversing a resonance. Resonances at $n = 0.5$, 0.36, 0.25, and 0.20 have been investigated.

1. Introduction

Betatron amplitude growth has been observed under certain conditions during the compression cycle of an electron ring accelerator [1,2]

† Work supported by the U.S. Atomic Energy Commission.

To better understand this phenomenon, and to be able to predict betatron-amplitude growth in future experiments, we undertook computer and analytical calculations pertaining to the device of ref. 2). In previous work with betatron resonances analytic[3-5] and some limited computer calculations[6] have been performed for other geometries. For an electron ring accelerator, the electrons typically are injected with a magnetic field index $n = (-r/B_z)(dB_z/dr)$ of about 0.5, and then during the compression cycle n decreases to ≈ 0.1.

Betatron resonant growth can occur when the radial oscillation frequency of an electron divided by its gyrofrequency, ν_r, or the axial oscillation frequency, divided by its gyrofrequency, ν_z, is a simple fraction, or when the ν_r and ν_z values are connected by simple integral relations. The quantities ν_r and ν_z are also called the radial and axial betatron tunes, and they are approximately related to the field gradient index n by

$$\nu_r^2 = 1 - n,$$
$$\nu_z^2 = n. \tag{1}$$

A particular resonance is designated by an equation of the form

$$k\nu_r + \ell\nu_z = m, \tag{2}$$

where k, ℓ, and m are positive or negative integers. In eq. (2) m indicates the harmonic order of the magnetic field's azimuthal variation that drives the resonance (see section 4). Important resonances arise when k, ℓ, and m are small, and if the magnetic field has median-plane symmetry, only resonances with even ℓ can occur.

We have investigated the following potentially dangerous resonances:

$$2\nu_r - 2\nu_z = 0, \quad \text{at} \quad n = 0.5;$$
$$\nu_r + 2\nu_z = 2, \quad \text{at} \quad n = 0.36;$$
$$2\nu_z = 1, \text{ at} \quad n = 0.25;$$
$$\nu_r - 2\nu_z = 0, \text{ at} \quad n = 0.20. \qquad (3)$$

Presumably less important, and hence not included in eqs. (3), are higher-order resonances and those occurring in fields with non-median-plane symmetry. Unless the magnetic field has large higher harmonic components, the growth will be greatest on the lower-order resonances. With regard to resonances that arise only in the absence of median-plane symmetry, electron ring compressors are designed with due consideration to median-plane symmetry, and magnetic measurements indicate that deviation from this symmetry is small.

In sections 2 and 3 we discuss the computer method of calculating betatron growth by simulating the experimental magnetic fields. Then, in section 4 the analytic method is discussed, in which growth is calculated from certain parameters that characterize the radial and (possible) azimuthal variations of the magnetic field and can be determined from the magnetic measurements. (Often these field parameters can be estimated from simple calculations.) After determining these field variations, one can use the convenient analytic formulas given in section 4 to predict the growth for each resonance. The growth rates calculated from these formulas when compared with the computer calculations have agreed typically within 30% and in the worst case within a factor of 2.

2. Computer Simulation of the Experimental Magnetic Field

To compute the effect of a betatron resonance on a particle, one must simulate closely the driving terms of the actual magnetic field.

It is convenient to separate the magnetic field into two parts: (a) an azimuthally symmetric field and (b) an azimuthally varying (perturbation) field (if it is of significant magnitude). Note that a non-symmetric field is not required to actuate a homogeneous ($m = 0$) resonance. For each particular calculation two arrays are stored in the computer. One array contains the axial and radial magnetic field components (B_z, B_r) for the symmetric field and the other array is used to calculate the nonsymmetric field (B_z, B_r, B_θ).

The computational results reported in this paper were obtained for fields intended to simulate those present in the compression experiments reported in ref. 2).

2.1 Symmetric Field

The experimental apparatus for forming rings usually contains three or four sets of compression coils (see fig. 1 of ref.2). The coils of ref.2) have many turns of copper windings. If the particle is 20 cm or further from the coil, the windings can be accurately simulated by infinitesimal circular current loops. The fields from these loops can then be calculated by integration of the Biot-Savart law[7]. If the particle is closer than about 20 cm to the coil, however, the helical nature and crossover region of the windings can alter the magnetic field; see section 2.2.

The coils in the apparatus of ref. 2) were pulsed, so that the currents used in the program could be taken from those measured experimentally with Rogowski belts. Alternatively they could be calculated from knowledge of the voltages and capacity of the capacitor banks, and the inductance, mutual inductance, and resistances of the coil system. Both methods gave essentially the same result, so the latter method usually was used.

Because of the pulsed nature of the fields, the magnetic field from one coil could induce eddy currents in the copper turns (whether shorted or unshorted) of another coil. For a shorted loop, the current induced in the complete circuit can be calculated in a rather direct manner. However, the induced eddy currents due to the physical presence of the copper even when the coil is open must also be included. This was taken into account in computation of the symmetric field by means of simulation circuits comprised of two adjacent current loops with current in opposite directions. The currents in these loop pairs (which were driven by the active coils) were calculated in the program after parameters, such as the mutual inductances to the main coils, were adjusted so that the resulting magnetic field gradients were in agreement with measured values.

The calculated symmetric magnetic field agreed very well with measured field, the difference being less than 2%.

2.2 Azimuthally Varying Fields

Azimuthal variations of magnetic fields arise from two sources: (a) asymmetric coil construction or location, (b) eddy currents in metal that is nonazimuthally symmetric and in spatially localized ferromagnetic material.

The coils were placed very accurately with regard to center and tilt, and the possible field perturbation from this effect was estimated to be small. The effect of coil leads was also calculated. This introduced a field asymmetry of only 0.1% in the midplane B_z.

Coil Sets 1B, 2, and 3 (see fig. 1 of ref. 2) were wound with a threefold symmetry in their crossovers (inner radius to outer radius). This minimized first and second harmonic perturbations but introduced

a third harmonic variation. The magnitude of this effect was calculated for a current element with the geometry of the crossover conductor, and the resultant axial field was 0.5 to 1% of the total symmetric field. During the first stage of compression only Coil Sets 1A and 1B were energized, but eddy currents in the unshorted copper crossovers of Coil Sets 2 and 3 produced field perturbations of the same magnitude as those arising from the normal currents in the crossovers in Coil Set 1B.

Eddy currents in the copper-iron injection snout[2], the stainless steel flanges, probe housing, etc. gave rise to large peripheral bumps in the magnetic field. Fig. 1 shows the azimuthal variation of the axial field component in the median plane for two radii at the time of injection. Similar data were obtained as a function of time for several radii from 11 cm to 19 cm. Also direct midplane measurements of $(\Delta B_z/\Delta r)$ were made.

The third harmonic component was described by the calculated field contribution from the crossovers. In addition, four circular current loops (and a bias field) were used to simulate the peripheral bumps. The radius and location of each loop were chosen to fit the width and radial variation of the measured bump. The currents in the four simulation loops were determined as a function of time by a least-squares fit of the calculated fields $B_z(r, \theta, z = 0, t)$ to the measured midplane fields. A typical example of such a calculated field at injection time for $R = 19$ cm is shown in fig. 2. At injection time the guide field was typically 700 G.

The compressor was designed to have median-plane symmetry in its magnetic field during the compression cycle. Although Coil Set 3 was mechanically unsymmetric, the turn-to-turn spacing in the short coil

of the pair was made larger so that the total field had reasonably good median-plane symmetry. Measurement of B_r indicated that the deviations from median-plane symmetry were small. Therefore, in the calculations it was assumed that B_r, and B_θ are zero on the median plane. For convenience, a midplane array of $B_z(r, \theta, z = 0, t_1)$ was stored in the computer for the orbit code to calculate resonant growth near a time t_1. If B_z on the midplane is known, $\underset{\sim}{B}$ can be calculated for small (z/r) by the expansion equations

$$B_z(z) = B_z\Big|_{z=0} - \frac{z^2}{2r^2}\left\{r\frac{\partial B_z}{\partial r}\Big|_{z=0} + r^2\frac{\partial^2 B_z}{\partial r^2}\Big|_{z=0} + \frac{\partial^2 B_z}{\partial \theta^2}\Big|_{z=0}\right\},$$

$$B_r(z) = z\frac{\partial B_z}{\partial r}\Big|_{z=0},$$

$$B_\theta(z) = \frac{z}{r}\frac{\partial B_z}{\partial \theta}\Big|_{z=0}. \qquad (4)$$

Most of the calculations were done neglecting the higher-order second term of B_z, as this simplification was found not to affect the results for those cases that were compared.

Another method of handling the azimuthally asymmetric field was to make a least-squares fit of the data (B_z and $\Delta B_z/\Delta r$) to Fourier series. For a particular time (when the resonance is crossed) arrays (C_m^B, S_m^B, C_m^P, S_m^P) of Fourier coefficients (vs. r) are stored in the computer for use by the orbit code. The components of the asymmetry field are calculated from the arrays as follows:

$$B_z(r,z,\theta) = \sum_m \left\{\left(1 + \frac{m^2 z^2}{2r^2}\right)\left[C_m^B(r)\cos m\theta + S_m^B(r)\sin m\theta\right]\right\}$$

$$- \frac{z^2}{2r}\sum_m\left[\left\{\frac{d}{dr}C_m^P(r)\right\}\cos m\theta + \left\{\frac{d}{dr}S_m^P(r)\right\}\sin m\theta\right],$$

$$B_r(r,z,\theta) = \frac{z}{r}\sum_m\left[C_m^P(r)\cos m\theta + S_m^P(r)\sin m\theta\right],$$

$$B_\theta(r,z,\theta) = \frac{z}{r}\sum_m m\left[S_m^B(r)\cos m\theta - C_m^B(r)\sin m\theta\right], \qquad (5)$$

where C_m^B and S_m^B are the Fourier coefficients determined from the midplane B_z measurements. The coefficients C_m^P and S_m^P represent respectively $r\frac{\partial}{\partial r}C_m^B$ and $r\frac{\partial}{\partial r}S_m^B$, and are determined directly from the midplane $\Delta B_z/\Delta r$ measurements.

3. Computer and Some Experimental Results for Betatron Amplitude Growth

A typical calculated compression cycle is plotted in fig. 3 to indicate how the radius R, magnetic field B, kinetic energy T, and magnetic field index n vary with time. The variation with time of n at the location of the closed orbit (as on fig. 3) we will call the "n trajectory." Trajectories similar to this could be calculated for any set of parameters used in the experiment.

The n value at the location of the closed orbit could be shifted experimentally by putting a small current through a coil set which by itself would cause a large value of n at that location. For example, a small capacitor (of an n-shifter circuit) could be discharged through Coil Set 1B (see fig. 1 of ref. 2) to shift the n trajectory at large radius.

By use of the exact relativistic equations of motion and a simulated magnetic field for which the characteristics were adjusted to fit the experimental conditions, the resulting particle motion was determined by numerical integration. To obtain a scan of the total interesting region of n, particles were injected with different energies at various appropriate radii into a magnetic field that was constant with time. They were injected with an axial amplitude of 0.1 cm and a radial amplitude of roughly 2 cm. The resulting axial amplitude growth rate for the particles is plotted in fig. 4. The computer results thus demonstrate directly that there are regions of growth near $n = 0.20$, 0.25, 0.36, and 0.50. The peaks are not exactly centered about these n values, because the axial motion is modified by radial motion of appreciable amplitude. If the same calculations are performed for an azimuthally symmetric field, the $n = 0.25$ and $n = 0.36$ peaks disappear, but the $n = 0.20$ and $n = 0.5$ peaks remain.

That these results have physical significance is demonstrated in fig. 5, which depicts the experimental results for a compression cycle during which n was rapidly swept over a large range. (This result was obtained with an experimental apparatus similar to that of ref. 1.) The X-ray signal is due to electrons striking an obstacle at 1.7 cm from the median plane and so is indicative of the acquisition of considerable axial amplitude. The value of n versus time was determined by a computer calculation and is accurate only to about 0.03. Thus, experimentally, there appear to be axial losses near $n = 0.5$, 0.25, and 0.20, in qualitative agreement with the computer calculations. (Axial growth near $n = 0.36$ has been observed for other conditions, but apparently it was too small to be observed in this case.)

The phenomenon of interest here in each case evidently is basically that which was treated in ref. 4). Briefly, in any resonant region an initially small axial amplitude exhibits an exponential growth, at least until quite large amplitudes are attained. The rate of this growth is dependent upon the proximity of n to the resonant value, and, in the case of coupling resonances, is dependent upon the amount by which the initial radial amplitude exceeds a certain threshold value.

To determine the total growth that would be expected in the operation of a compressor, it is necessary to traverse the resonance in the course of the computation. To simplify the calculation, the arrays for the symmetric and azimuthally asymmetric fields are stored in the computer for approximately the time at which a particular resonance is crossed. Then the symmetric magnetic field and the particle energy are varied with time at the same rate as they change during compression.

3.1 $2\nu_r - 2\nu_z = 0$ ($n = 0.50$) Resonance

This resonance occurs in the absence of azimuthal bumps, and is driven by nonlinearities of the field $(\partial^2 B_z/\partial r^2)$, $(\partial^3 B_z/\partial r^3)$, etc. This was shown in the computer calculations by runs with and without azimuthal bumps and with several different values of $(\partial^2 B_z/\partial r^2)$ and $(\partial^3 B_z/\partial r^3)$.

An example of crossing this resonance during the experiment[2)] is shown in fig. 6. The x-ray signal is due to an axial loss of electrons when the n trajectory crossed $n = 0.5$. By moving the ring into a probe at smaller radius it was determined that about 1/3 of the electrons were lost on this resonance.

A computer simulation of traversing this resonance is shown in fig. 7. The particle is followed for only the few microseconds during which the resonance is traversed. The variation of n with number of revolutions (or time) is shown at the top of fig. 7. The time for one revolution is about 3.5 nsec.

Since the particle's position is not always printed out for its maximum axial or radial excursion, it is convenient to take for the axial and radial amplitudes the quantities

$$A_z = [(p_z/m_0\gamma\omega_{ce})^2/n + z^2]^{1/2} \tag{6}$$

and

$$A_r = [(p_r/m_0\gamma\omega_{ce})^2/(1-n) + (r - R)^2]^{1/2}, \tag{7}$$

where p_z and p_r are the momentum components, m_0 is the electron rest mass, γ is the ratio of total mass to rest mass, ω_{ce} is the gyrofrequency, and R is the radius of the closed orbit. By tracking particles in a constant magnetic field, R can be determined for a given electron energy. However, in traversing a resonance, R changes with time. Since $R \approx r_{ave}$ and r_{ave} is easier to obtain in the computer calculation, r_{ave} was used for most of the calculations of A_r. The initial radial and axial betatron amplitudes were chosen, for this calculation, to be 1.5 cm and 0.1 cm, respectively (see fig. 7). As one can see, the axial amplitude grows while the radial amplitude decreases. Several different initial phases were tried with similar results. Also the initial radial amplitude was varied, and in each case the axial amplitude grew to equal the initial radial amplitude. Because of the multiturn injection process, the initial radial amplitudes are 2 to 3 cm, and particles strike the walls if the axial

amplitudes grow to greater than about 2 cm. Thus this resonance growth at $n = 0.5$ explains the X-ray signals of fig. 6.

If a particle is injected into a constant magnetic field in the middle of the resonance, the axial and radial amplitudes continuously exchange maxima and minima, as shown in fig. 8. From these and other computer calculations an approximate rule for the relationship between axial and radial amplitudes was obtained,

$$A_z^2 + A_r^2 \approx \text{const.} \tag{8}$$

This rule seems to fit very well for small and moderate amplitudes. However, if the amplitudes become extreme, the rule breaks down. The maximum growth rate was shown to be approximately proportional to A_r^2.

3.2 $\nu_r - 2\nu_z = 0$ ($n = 0.20$) Resonance

This resonance at $n = 0.2$ is often referred to as the Walkinshaw resonance[3]. It has many similarities to the ($2\nu_r - 2\nu_z = 0$) resonance discussed in 3.1. This resonance also can be driven by nonlinearities of the magnetic field in the absence of azimuthal variations.

The relationship between axial and radial amplitudes for this resonance is[5]

$$A_z^2 + 4A_r^2 \approx \text{const}, \tag{9}$$

for small and moderate amplitudes. This is demonstrated by the computational results, plotted in fig. 9, for particle motion in a constant magnetic field for which n has the resonant value 0.2. The maximum growth rate is approximately proportional to A_r.

3.3 $2\nu_z = 1$ ($n = 0.25$) Resonance

This resonance was shown to be driven by azimuthal asymmetries

of the magnetic field. It was further shown by decomposing the field into its Fourier components that just first harmonic variations drive this resonance. Calculations were done for several initial values of A_r with no indication that the growth rate depends on A_r.

3.4 $\nu_r + 2\nu_z = 2$ (n = 0.36) Resonance

This resonance was shown to be driven by azimuthal asymmetries of the magnetic field. It was further shown by decomposing the field into its Fourier components that second harmonic variations account for more than 80% of the observed growth rate in typical cases. Also, the growth rate was shown to be roughly proportional to A_r.

In determining the total growth developed in traversing this resonance it was particularly important to start particles with several different phases. The sensitivity of the accumulated growth to the initial phase of the axial motion may be attributed to the fact that this resonance is inhomogeneous ($m \neq 0$) and involves a coupling effect from the radial motion. (The choice of the otherwise arbitrary origin of the angular coordinate θ cannot be used effectively in such cases to eliminate the apparent significance of phase differences between radial motion, axial motion, and the field perturbations.) Some particles have an increase in betatron amplitude, whereas other particles have a decrease. In fig. 10 the axial momentum p_z and position z are plotted for 24 particles (with different initial phases) for different times as the resonance is traversed. "T" refers to the number of revolutions (gyroperiods). One notes from fig. 10 that the elongation of the phase-space ellipses means that, after the resonance has been traversed, most particles have a larger axial betatron amplitude whereas some particles have a smaller axial amplitude.

4. Analytical Formulas for Four Resonances

The derivations of the analytical expressions for the growth rate, total growth, and width are given in Appendix A for the resonances described in section 3. The results of these calculations are given below. For the $2\nu_z + \nu_r = 2$ (n = 0.36) resonance and the $2\nu_z = 1$ (n = 0.25) resonance it was assumed that the midplane magnetic field had the form

$$B_z = B_0(r) + \sum_m [C_m(r,t) \cos m\theta + S_m(r,t) \sin m\theta]. \tag{10}$$

The resonances do not always occur exactly at the expected value of n (see fig. 4) because of the modification of the axial equation by radial motion of appreciable amplitude.

4.1 $2\nu_r - 2\nu_z = 0$ (n = 0.50) Resonance

Let

$$b'' = \frac{R^2}{B_0} \left. \frac{\partial^2 B_z(r,t)}{\partial r^2} \right|_{r=R},$$

$$b''' = \frac{R^3}{B_0} \left. \frac{\partial^3 B_z(r,t)}{\partial r^3} \right|_{r=R}, \tag{11}$$

where R and t are the radius and time at which the resonance is crossed. Then the maximum growth rate, total growth, growth factor, and full width of the resonance are given by

$$M = \text{Maximum Growth Rate} = \frac{0.020\, A_r^2}{R^2} \left| 3 + 20b'' - 56b''^2 - 12b''' \right| \quad \text{(decades/rev)}, \tag{12}$$

$$G = \text{Total Growth} = \frac{1.6 \times 10^{-4} A_r^{\,4}}{R^4} \quad \frac{[3 + 20b'' - 56b''^2 - 12b''']^2}{|dn/d(\text{rev})|} \quad (\text{decades}), \tag{13}$$

$$\text{Growth Factor} = 10^G, \tag{14}$$

and

$$\Delta n = 0.52\ M, \tag{15}$$

where A_r is the radial betatron amplitude given by eq. (7), and $dn/d(\text{rev})$ (the change in n per revolution) measures the rate at which the resonance is crossed. Thus for a given initial axial betatron amplitude, the predicted axial betatron amplitude after traversing the resonance is given by

$$A_z(\text{final}) = 10^G\ A_z\ (\text{initial}). \tag{16}$$

If the value for the final A_z [calculated by eq. (16)] is greater than A_r, then, in general, the limitations on growth given in eq. (8) will apply.

To minimize the growth caused by traversing this resonance one wishes to minimize the quantity $(3 + 20b'' - 56b''^2 - 12b''')$. Fig. 11 shows the curve of the equation

$$3 + 20b'' - 56b''^2 - 12b''' = 0. \tag{17}$$

This relation between b'' and b''' for minimum growth was checked with a computer code using approximate equations of motion, and the four points obtained by minimizing growth for a given b'' are also plotted in fig. 11. Results with exact particle trajectories were also consistent with this curve.

4.2 $\nu_r - 2\nu_z = 0$ ($n = 0.20$) Resonance

Here one has

$$M = \text{Maximum Growth Rate} = \frac{1.5 A_r}{R}\ |b''|\ (\text{decades/rev}), \tag{18}$$

$$G = \text{Total Growth} = \frac{0.96}{|dn/d(\text{rev})|} \left(\frac{A_r b''}{R}\right)^2 \ (\text{decades}), \tag{19}$$

$$\text{Growth Factor} = 10^G, \tag{20}$$

and

$$\Delta n = 0.52\ M. \tag{21}$$

If the value for the final A_z [calculated by eq. (16)] is greater than $2A_r$, then, in general, the limitations on growth given in eq. (9) will apply.

4.3 $2\nu_z = 1$ ($n = 0.25$) Resonance

Let

$$C'_m(r,t) = r\ \frac{\partial C_m(r,t)}{\partial r}\ ,$$

$$S'_m(r,t) = r\ \frac{\partial S_m(r,t)}{\partial r}\ , \tag{22}$$

and

$$K = \frac{1}{B_0} \left\{ [2C_1(r,t) - C'_1(r,t)]^2 - [2S_1(r,t) - S'_1(r,t)]^2 \right\}^{1/2}, \tag{23}$$

where C_m, S_m, and B_0 are defined by eq. (10). Then,

$$M = \text{Maximum Growth Rate} = 1.4\ K\ (\text{decades/rev}), \tag{24}$$

$$G = \text{Total Growth} = \frac{1.1\ K^2}{|dn/d(\text{rev})|}\ (\text{decades}), \tag{25}$$

$$\text{Growth Factor} = 10^G \tag{26}$$

and

$$\Delta n = 0.73\ M. \tag{27}$$

4.4 $\nu_r + 2\nu_z = 2$ (n = 0.36) Resonance

Let

$$C_m'' = \frac{\partial}{\partial r}\left[r^2 \frac{\partial C_m(r,t)}{\partial r}\right],$$

$$S_m'' = \frac{\partial}{\partial r}\left[r^2 \frac{\partial S_m(r,t)}{\partial r}\right], \tag{28}$$

and

$$L = \frac{1}{2B_0}\left[(C_2'')^2 + (S_2'')^2\right]^{1/2}, \tag{29}$$

where C_m, S_m and B_0 are defined by eq. (10). Then

$$M = \text{Maximum Growth Rate} = 1.1\ \frac{A_r}{R}\left|L\right| \quad \text{(decades/rev)}, \tag{30}$$

$$G = \text{Total Growth} = \frac{1.4\ A_r^2 L^2}{R^2\left|dn/d(\text{rev})\right|} \quad \text{(decades)}, \tag{31}$$

$$\text{Growth Factor} = 10^G \tag{32}$$

and

$$\Delta n = 1.4\ M. \tag{33}$$

It should be noted that the formulas above apply for the particle with the maximum growth on the phase-space ellipse (see fig. 10).

5. Discussion

To understand the resonant growth behavior observed in experiments during the compression phase of an electron ring accelerator, computer and analytical calculations have been performed for conditions similar to those in the experiment of ref. 2). At low intensity, when only single-particle effects should be important, the calculations agree

qualitatively with the experimental results. At high intensity some energy spreading occurs that broadens the time at which different particles cross the resonance. This makes it more difficult to compare the experimental and computer results, but even in these cases they seem to be consistent.

The calculations have also elucidated the driving terms for each resonance. Thus, if a particular resonance causes large growth one can try to reduce the field variation driving that resonance. For the n = 0.5 and n = 0.2 resonances one could add extra coils to adjust b" and b"' at the time the resonance is crossed. Changing the coil spacing or energizing the coils in a different sequence also can affect b" and b"'. For the n = 0.36 and n = 0.25 resonances the significant perturbations are greatest near the periphery of the chamber. By use of an n-shifter circuit these resonances can be crossed at smaller radii where the perturbations are smaller. If the magnetic-field bumps are still too large, one can remove various components from or add them to the simulated field in a computational program until satisfactory growth is obtained. Then one could remove these same components from (or add them to) the real experimental apparatus.

Looking at the formulas for "total growth" one notes that the total growth is proportional to the factor $1/\left|dn/d(\text{rev})\right|$. Thus if a resonance can be crossed more rapidly this, in general, will reduce the growth, particularly since it appears in the exponent of the "growth factor." This will work well if the growth is not too large. For the n = 0.5 and n = 0.2 resonances, if the growth is so large that it is already limited only by the initial radial betatron amplitude, a small change in the speed of crossing the resonance may not

reduce the final axial amplitudes.

ACKNOWLEDGMENTS

We are very appreciative for the use of the results of magnetic measurement performed by J. M. Peterson and J. B. Rechen. We are very thankful to A. C. Paul for a modified version of his orbit code and to D. R. George for his help in cataloging the measured and computed data. Helpful discussions with J. M. Peterson, A. M. Sessler, D. Keefe, and G. R. Lambertson are gratefully acknowledged.

APPENDIX A

Derivation of Analytical Formulas of Section 4

These calculations are directed to the occurrence of a substantial exponential growth of axial amplitude when the radial amplitude is sufficiently great. The axial amplitude is assumed to be small initially, consequently the axial motion can be characterized by a linear differential equation in which the radial motion may be regarded as a prescribed function.

The general procedure for deriving the analytical formulas is

(a) Determine the radial and axial equations of motion for a particle in the magnetic field.

(b) Determine an appropriate expression for the magnetic field which contains the relevant driving terms for the particular resonance under consideration. Then put this magnetic field into the equations of motion of (a).

(c) Make reasonable approximations to obtain a simple expression for the radial coordinate with the axial coordinate ignored. Then insert this expression into the axial equation of motion.

(d) After confirming that the axial equation has the form of a Hill or Mathieu equation, obtain a simple approximate solution.

(e) Using this solution, determine the width of the stop band of the resonance, the maximum growth rate, and the total growth.

We obtain the equations of motion from the Principle of Least Action,

$$\delta \int (\underset{\sim}{p} - e\underset{\sim}{A}) \cdot d\underset{\sim}{s} = 0, \qquad \text{(A1)}$$

where $\underset{\sim}{p}$ is the mechanical momentum and $\underset{\sim}{A}$ is the vector potential.

Since $d\underset{\sim}{s} = (r'\hat{e}_r + z'\hat{e}_z + r\hat{e}_\theta)d\theta$ (where the primes indicate differentiation with respect to θ), eq. (A1) can be expressed as

$$\delta \int\{ p[r^2 + r'^2 + z'^2]^{\frac{1}{2}} - e[rA_\theta + r'A_r + z'A_z]\} \, d\theta = 0 . \qquad \text{(A2)}$$

In the median plane, the radial variation of (A2) gives the familiar trajectory equation,

$$\frac{d}{d\theta}\left[\frac{pr'}{(r^2 + r'^2)^{\frac{1}{2}}}\right] - \frac{pr}{(r^2 + r'^2)^{\frac{1}{2}}} + e\left(\frac{\partial(rA_\theta)}{\partial r} - \frac{\partial A_r}{\partial \theta}\right) = 0, \qquad \text{(A3)}$$

or

$$\frac{d}{d\theta}\left[\frac{pr'}{(r^2 + r'^2)^{\frac{1}{2}}}\right] = \frac{pr}{(r^2 + r'^2)^{\frac{1}{2}}} - erB_z .$$

For $r' \ll r$ this can be written as the simplified approximate equation

$$r'' - r + er^2 B_z/p = 0. \qquad \text{(A4)}$$

Considering the axial variation of (A2) results in

$$\frac{d}{d\theta}\left[\frac{pz'}{(r^2 + r'^2 + z'^2)^{\frac{1}{2}}}\right] - er\left(\frac{1}{r}\frac{\partial A_z}{\partial \theta} - \frac{\partial A_\theta}{\partial z}\right) + er'\left(\frac{\partial A_r}{\partial z} - \frac{\partial A_z}{\partial r}\right) = 0, \qquad \text{(A5)}$$

or

$$\frac{d}{d\theta}\left[\frac{pz'}{(r^2 + r'^2 + z'^2)^{\frac{1}{2}}}\right] = erB_r - er'B_\theta ,$$

which similarly may be approximated as

$$z'' - er^2 B_r/p = 0. \qquad \text{(A6)}$$

1. $\nu_r - 2\nu_z = 0$ $(n = 0.20)$ Resonance

Because the relation between the oscillation frequencies is homogenous [it has the form of eq. (2) with $m = 0$], azimuthal field variations are not required for excitation of this resonance, and it therefore is appropriate to focus attention instead on the effect of nonlinearity in the magnetic field.

Let

$$x = \frac{r-R}{R}$$

and $\qquad \text{(A7)}$

$$y = \frac{z}{R} .$$

Expanding the magnetic field about $r = R$ and $z = 0$, with B_z symmetric with respect to the median plane, and using Maxwell's equation, we obtain

$$B_z = B_0 \, [1 - nx + \tfrac{1}{2}b'' \, (x^2 - y^2)] \ , \qquad \text{(A8)}$$

$$B_r = B_0 \, [- ny + b''xy] \ , \qquad \text{(A9)}$$

where b'' is given by eq. (11). Curvature effects have been neglected in (A8) and (A9), and these field components satisfy the curl condition $\frac{\partial B_z}{\partial x} = \frac{\partial B_r}{\partial y}$ and the divergence condition $\nabla \cdot \underset{\sim}{B} \approx \frac{1}{R}\left[\frac{\partial B_r}{\partial x} + \frac{\partial B_z}{\partial y}\right] = 0.$

Substituting (A8) and (A9) into (A4) and (A6) and neglecting higher-order terms results in

$$x'' + (1-n)x - \tfrac{1}{2}b''\,(y^2 - x^2) = 0 \qquad \text{(A10)}$$

and

$$y'' + ny - b''xy = 0\,, \qquad \text{(A11)}$$

where we have used eq. (A7) and $p = eRB_0$.

We adopt the viewpoint of Walkinshaw[3] and treat the x motion as a prescribed motion unaffected by coupling effects. This non-Hamiltonian approach appears to be entirely justified when one is examining the onset of y growth from initial amplitudes that are quite small.

In this spirit one writes eq. (A11) as

$$y'' + (\nu_y^{\,2} - b''x)y = 0 \qquad \text{(A12)}$$

and introduces† $x = A_x \cos \nu_x\theta$ to obtain the Mathieu equation

$$y'' + (\nu_y^{\,2} - b''A_x \cos \nu_x\theta)y = 0, \qquad \text{(A13)}$$

where $\nu_x^{\,2} = 1-n$ and $\nu_y^{\,2} = n$.

The relevant "stop band" for this equation, within which growth ultimately will occur for all non zero initial conditions (save for a set of measure zero) is defined by the inequalities††

† An additional phase constant in the expression for x would clearly be inconsequential in this case, as it would correspond to no more than a translation of the origin of θ.

†† See ref. 4), esp. eqs. (2.7) and (2.9), p. 1237. These expressions are, of course, merely the leading terms of well-known series developments for the eigenvalues associated with the eigenfunctions ce_1 and se_1 of the Mathieu equation [cf. Whittaker and Watson, Modern Analysis (Cambridge University Press, London and New York, 1927), Sect. 19.3]. The phase shift of these solutions, per period of the coefficient of y, is π (and hence $\nu_y \approx \nu_x/2$).

$$\frac{\nu_x^{\,2}}{4} - \left|\frac{b''A_x}{2}\right| < \nu_y^{\,2} < \frac{\nu_x^{\,2}}{4} + \left|\frac{b''A_x}{2}\right| \;; \qquad \text{(A14)}$$

i.e., by†

$$\left|\nu_x^{\,2} - (2\nu_y)^2\right| < 2\left|b''A_x\right|\,, \qquad \text{(A15)}$$

or

$$\left|A_x\right| > A_{thr} = \frac{\left|\nu_x^{\,2} - (2\nu_y)^2\right|}{2\left|b''\right|}\,. \qquad \text{(A16)}$$

The quantity A_{thr} defined by eq. (A16) thus constitutes a threshold amplitude of radial motion above which axial growth will be expected to occur.

Within the stop-band just defined one expects a lapse rate μ, for the amplitude of the exponentially growing solution of the Mathieu equation (A13), given by††

$$\mu \approx \left\{\frac{\left[\nu_y^{\,2} - \left(\frac{\nu_x}{2}\right)^2 - \frac{1}{2}\,b''A_x\right]\left[\left(\frac{\nu_x}{2}\right)^2 - \frac{1}{2}\,b''A_x - \nu_y^{\,2}\right] < c^2 > < s^2 >}{4 < -sc' > < cs' >}\right\}^{1/2}. \qquad \text{(A17)}$$

For the eigenfunctions $c(\theta)$ and $s(\theta)$, it is convenient merely to take $\cos \nu_y\theta$ and $\sin \nu_y\theta$ respectively, resulting in

$$\frac{\langle c^2\rangle\,\langle s^2\rangle}{\langle -\,sc'\rangle\,\langle cs'\rangle} \approx \frac{1}{\nu_y^{\,2}}\,. \qquad \text{(A18)}$$

Then,

$$\mu = \frac{\left|b''\right|}{4\nu_y}\,(A_x^{\,2} - A_{thr}^2)^{1/2} \text{ neper per radian of } \theta. \qquad \text{(A19)}$$

† Cf. section IIIA of ref. 4, especially eqs. (3.4) and (3.5), pp. 1241-1242, with $a = \nu_y^{\,2}$, $b = c = 0$, and $d = -b''A_x$.

†† Ref. 4, section IID, especially eq. (2.58), p. 1240.

Writing $A_x = A_r/R$ and $\nu_y \approx \sqrt{0.2}$, with $A_{thr} = 0$, we obtain the maximum growth rate

$$M = \frac{\pi}{\sqrt{0.8}\,\ln 10}\,\frac{A_r}{R}\,|b''| \quad \text{decades/rev} . \tag{A20}$$

In passage through the resonance there is an accumulated growth that can be estimated by use of eq. (A17), which is conveniently rewritten as

$$\mu = [(2b''A_x - 1 + 5n)(2b''A_x + 1 - 5n)]^{1/2}/(8\sqrt{0.2}). \tag{A21}$$

In passage through the resonance, n increases from its value

$$n_1 = \frac{1 - 2|b''|A_x}{5} \tag{A22}$$

at one edge of the stop band to

$$n_2 = \frac{1 + 2|b''|A_x}{5} \tag{A23}$$

at the other. On the assumption that the growth is not so great that turnover has occurred or is approached, the y amplitude is expected to grow by the factor $\exp\int_{n=n_1}^{n=n_2}\mu d\theta$. If the resonance is traversed at a constant rate of change of $n\left[\frac{dn}{d\theta} = \text{const.}; \text{ or } \frac{dn}{d\theta} = \frac{1}{2\pi}\frac{dn}{d(\text{rev})}\right.$, where $\frac{dn}{d(\text{rev})}$ is the rate of change of n per revolution and is treated as a constant$\left.\right]$, one has

$$\int_{n=n_1}^{n=n_2}\mu d\theta = \frac{1}{\left|\frac{dn}{d\theta}\right|}\int_{n_1}^{n_2}\mu dn = \frac{2\pi}{\left|\frac{dn}{d(\text{rev})}\right|}\int_{n_1}^{n_2}\mu dn$$

$$= \frac{2\pi}{\left|\frac{dn}{d(\text{rev})}\right|}\int_{n_1}^{n_2}\frac{5\sqrt{(n-n_1)(n_2-n)}}{8\sqrt{0.2}}\,dn = \frac{(\pi^2/4)(5/4)^{3/2}(n_2-n_1)^2}{|dn/d(\text{rev})|}$$

$$= \frac{\pi^2}{2\sqrt{5}}\,\frac{b''^2 A_x^2}{|dn/d(\text{rev})|} \quad \text{nepers}, \tag{A24}$$

or the total growth is

$$G = \frac{\pi^2}{2\sqrt{5}\,\ln 10}\,\frac{1}{|dn/d(\text{rev})|}\left(\frac{A_r b''}{R}\right)^2 \quad \text{decades}. \tag{A25}$$

The width of the resonance is

$$\Delta n = |n_2 - n_1| = \frac{4A_r}{5R}|b''| = \frac{8\sqrt{0.2}\,\ln 10}{5\pi}\,M \approx 0.52\,M. \tag{A26}$$

2. $2\nu_r - 2\nu_z = 0$ ($n = 0.50$) Resonance

Here also the relation between the oscillation frequencies is homogeneous, and it again is appropriate to focus attention on the effect of nonlinearity in the magnetic field.

The resonance $2\nu_r - 2\nu_z = 0$ is of higher order than most of the coupling resonances to which attention has been given, leading, for example, to a predicted "stop-band width" that is proportional to the square rather than to the first power of the radial amplitude. Special care must be taken, therefore, not to omit effects whose consequences would be of the same order as those treated in the analysis, and the

algebraic work correspondingly is tedious. The analysis presented below has, however, been subjected to some computational checks and is believed to constitute an adequate semiquantitative description of the axial growth that can arise from the $2\nu_r = 2\nu_z$ resonance.

The magnetic field can be adequately described by means of an azimuthally directed vector-potential function that is developed in terms of the coordinates x and y as†

$$\frac{rA_\theta}{R^2B_0} = \frac{2x + x^2}{2} - \frac{3x^2 + 2x^3}{6}n + \frac{4x^3 + 3x^4}{24}b'' + \frac{5x^4 + 4x^5}{120}b'''$$

$$+ \frac{1 + x}{2}\left(n - xb'' - \frac{1}{2}x^2b'''\right)y^2. \qquad \text{(A27)}$$

Here n is the field index, and b'', b''' are constants that have been evaluated at the (circular) equilibrium orbit of radius R [see eqs. (11)]. The differential equation for uncoupled radial motion (A3) with use of this vector potential is

$$\frac{d}{d\theta}\left[\frac{x'}{\sqrt{(1+x)^2+x'^2}}\right] - \frac{1+x}{\sqrt{(1+x)^2+x'^2}} + (1+x)\left[1-nx+\frac{1}{2}b''x^2+\frac{1}{6}b'''x^3\right] = 0, \qquad \text{(A28)}$$

where x' denotes $dx/d\theta$ and we have set $p = eRB_0$.

To provide in full measure the required alternating terms in the equation for axial motion, it is necessary to obtain a solution for x

† The expression given for rA_θ/R^2B_0 can be extended to a more consistent form by the addition of the term

$$\frac{1}{24(1+x)}\left(n + b'' + \frac{2 + 6x + 3x^2}{2}b'''\right)y^4;$$

such a term is not required for the present analysis, however, since only linear forces are included in the differential equation for axial motion used here.

that is valid through terms proportional to the square of the radial-oscillation amplitude. Terms proportional to x'^2 in the differential equation thus properly should not be ignored. A suitable solution, obtainable by harmonic balance, is of the form[8]

$$x = P_0 + P_1 \cos \nu_x\theta + P_2 \cos 2\nu_x\theta \qquad \text{(A29)}$$

(an inconsequential arbitrary phase constant being ignored), with

$$P_0 = \left(3C_2 + \frac{1}{4}\right)A_x^2, \quad P_1 = A_x, \quad P_2 = -\left(C_2 - \frac{1}{12}\right)A_x^2 \qquad \text{(A30)}$$

and

$$\nu_x^2 = 1 - n - \left(15\,C_2^2 + \frac{5}{4}C_2 + \frac{3}{4}C_3 - \frac{11}{96}\right)A_x^2; \qquad \text{(A31)}$$

here $C_2 = -(2-4n + b'')/6$ and $C_3 = (6n - 6b'' - b''')/6$, and these coefficients are approximately equal to $-\frac{1}{6}b''$ and $\frac{1}{2} - b'' - \frac{1}{6}b'''$, respectively, for $n \approx \frac{1}{2}$.

The linearized differential equation that describes small-amplitude axial excursions is obtained from eq. (A5):

$$\frac{d}{d\theta}\left[\frac{y'}{\sqrt{(1+x)^2 + x'^2}}\right] + (1+x)\left(n - b''x - \frac{1}{2}b'''x^2\right)y = 0, \qquad \text{(A32)}$$

with $y' = dy/d\theta$. The quantity $\left[(1+x)^2 + x'^2\right]^{-\frac{1}{2}}$ may now be expanded through terms of order x^2 or x'^2 and the solution previously given for x substituted into this equation to obtain a result of the form

$$\frac{d}{d\theta}\left[(1+\alpha_2+\beta_2\cos \nu_x\theta+\gamma_2\cos 2\nu_x\theta)y'\right] + (\alpha_0+\beta_0\cos \nu_x\theta+\gamma_0\cos 2\nu_x\theta)y=0, \qquad \text{(A33)}$$

where

$$\alpha_2 = (\tfrac{1}{8} + \tfrac{1}{2}b'')A_x^2 , \quad \beta_2 = - A_x , \quad \gamma_2 = (\tfrac{13}{24} - \tfrac{1}{6}b'')A_x^2 ,$$

$$\alpha_0 = n + (\tfrac{1}{8} - b'' + \tfrac{1}{2} b''^2 - \tfrac{1}{4} b''')A_x^2, \quad \beta_0 = (n-b'')A_x,$$

$$\gamma_0 = (\tfrac{1}{24} - \tfrac{1}{2}b'' - \tfrac{1}{6}b''^2 - \tfrac{1}{4}b \quad)A_x^2 . \tag{A34}$$

The differential equation (A33) can be regarded as a generalized Hill equation, for which we may seek eigenvalues α_0 that permit periodic solutions with a basic frequency (ν_y) equal to ν_x. It will be recognized that with regard to the coefficient γ_0 such solutions would be analogous to the solutions se_1 and ce_1 that occur at the boundaries of the first stop band for the Mathieu equation, whereas with respect to the coefficient β_0 they are analogous to the functions se_2 and ce_2 associated with the second stop band of the Mathieu equation. Because β_0 is directly proportional to A_x and γ_0 is proportional to A_x^2, one thus may expect that the influence of each of these terms will be to generate a stop band whose width is proportional to A_x^2.

By the use, in turn, of trial functions of the form $D_1 \sin \nu_x\theta + D_2 \sin 2\nu_x\theta$ and $E_0 + E_1 \cos \nu_x\theta + E_2 \cos 2\nu_x\theta$, the procedure of harmonic balance leads respectively to the following estimates for the corresponding eigenvalues:

$$\alpha_{0,1} = \nu_x^2 - \left(\tfrac{5}{32} - \tfrac{11}{24} b'' + \tfrac{1}{4} b''^2 + \tfrac{1}{8} b'''\right) A_x^2 ,$$

$$\alpha_{0,2} = \nu_x^2 - \left(\tfrac{7}{32} - \tfrac{1}{24} b'' - \tfrac{11}{12} b''^2 - \tfrac{1}{8} b'''\right) A_x^2 , \tag{A35}$$

or, after the expression given in Eq. (A31) for ν_x^2 is inserted,

$$\alpha_{0,1} = 1 - n - \left(\tfrac{5}{12} - \tfrac{17}{12}b'' + \tfrac{2}{3}b''^2\right)A_x^2 ,$$

$$\alpha_{0,2} = 1 - n - \left(\tfrac{23}{48} - b'' - \tfrac{1}{2}b''^2 - \tfrac{1}{4}b'''\right) A_x^2 . \tag{A36}$$

Finally, noting that

$$\alpha_0 = n + \left(\tfrac{1}{8} - b'' + \tfrac{1}{2}b''^2 - \tfrac{1}{4}b'''\right) A_x^2 , \tag{A37}$$

we obtain the estimated stability boundaries

$$n_1 = \frac{1}{2} - \frac{13 - 58b'' + 28b''^2 - 6b'''}{48} A_x^2 , \tag{A38}$$

$$n_2 = \frac{1}{2} - \frac{29 - 96b'' - 24b'''}{96} A_x^2 , \tag{A39}$$

with a central value

$$n_c = \frac{1}{2} - \frac{55 - 212b'' + 56b''^2 - 36b'''}{192} A_x^2 \tag{A40}$$

and a width

$$\Delta n = \left|n_2 - n_1\right| = \frac{\left|3 + 20b'' - 56b''^2 - 12b'''\right|}{96} A_x^2. \tag{A41}$$

Within the stop band bounded by the eigenvalues $\alpha_{0,1}$ and $\alpha_{0,2}$ one expects† that the growth rate of an exponentially increasing solution (formed approximately as $e^{\mu\theta}$ times a linear combination of

† See ref. 4, especially Sect. IID, p. 1240.

the periodic eigenfunctions associated with the boundaries of this stop band) will be given approximately by

$$\mu = \left(\frac{(\alpha_0-\alpha_{0,1})(\alpha_{0,2}-\alpha_0)}{4\nu_x^2}\right)^{\frac{1}{2}} = \left[0.5(\alpha_0-\alpha_{0,1})(\alpha_{0,2}-\alpha_0)\right]^{\frac{1}{2}} \text{ nepers/radian.} \tag{A42}$$

By use of the expressions previously given for α_0, $\alpha_{0,1}$, and $\alpha_{0,2}$, this characteristic exponent becomes

$$\mu = \left[2(n-n_1)(n_2-n)\right]^{\frac{1}{2}} \text{ nepers/radian,} \tag{A43}$$

with a maximum growth rate of

$$M = \frac{\sqrt{2}\,\pi}{96 \ln 10}\left|3 + 20b'' - 56b''^2 - 12b'''\right|\left(\frac{A_r}{R}\right)^2 \text{ decades/rev.} \tag{A44}$$

The total growth in traversing the resonance is

$$G = \int_{n=n_1}^{n_2} \mu d\theta = \frac{\pi^2 \sqrt{2}}{36864 \ln 10} \frac{(3+20b''-56b''^2-12b''')^2}{|dn/d(\text{rev.})|}\left(\frac{A_r}{R}\right)^4 \text{ decades.} \tag{A45}$$

The proportionality of this result to A_r^4, being characteristic of traversal of a second-order resonance, is noteworthy.

3. $2\nu_z = 1 (n = 0.25)$ Resonance

We represent the magnetic field components by expressions that contain azimuthal variations but are carried only through first-order terms in x, y. The radial motion in this case contains a flutter that arises from closed-orbit distortions produced by the azimuthal variation

of B_z, and this flutter is introduced into the axial equation through the factor $r^2[= R^2(1+2x + \cdots)]$ of eq. (A4). In principle a term of similar order would arise from the inclusion of the second-order term $B_0 b'' \cdot xy$ in B_r, but normally the contribution of this additional term is relatively small. We accordingly write

$$B_z = B_0(1-nx) + C_m^B \cos m\theta + S_m^B \sin m\theta + (C_m^P \cos m\theta + S_m^P \sin m\theta)\, x \tag{A46}$$

and

$$B_r = -\, n B_0 y + (C_m^P \cos m\theta + S_m^P \sin m\theta) y, \tag{A47}$$

where

$$C_m^P = \left[r \frac{dC_m^B(r)}{dr}\right], \qquad S_m^P = \left[r \frac{dS_m^B(r)}{dr}\right], \tag{A48}$$

with the coefficients C_m^B, S_m^B, C_m^P, S_m^P evaluated at $r = R$.

The resonance $2\nu_z = 1$ has the form of eq. (2) with $m = 1$, indicating that first harmonic variations in the azimuthal field are important. Substituting the magnetic field of eqs. (A46) and (A47), with $m = 1$, into eqs. (A4) and (A6) and neglecting higher-order terms in x and y results in

$$x'' + (1-n)x + x[(C_1^P + 2C_1^B)\cos\theta + (S_1^P + 2S_1^B)\sin\theta]/B_0 = -(C_1^B \cos\theta + S_1^B \sin\theta)/B_0, \tag{A50}$$

$$y'' + (1+2x)ny - (C_1^P \cos\theta + S_1^P \sin\theta)\,(y/B_0) = 0. \tag{A51}$$

In a low order of approximation, we write the solution to (A50) as

$$x \approx \frac{C_1^B \cos\theta + S_1^B \sin\theta}{nB_0} . \tag{A52}$$

Substituting (A52) into (A51), we obtain

$$y'' + ny + [(2C_1^B - C_1^P)\cos\theta + (2S_1^B - S_1^P)\sin\theta]\, y/B_0 = 0 . \tag{A53}$$

Thus we may consider the Hill equation

$$y'' + (n + K\cos\theta)y = 0, \tag{A54}$$

where

$$K = \frac{1}{B_0}[(2C_1^B - C_1^P)^2 + (2S_1^B - S_1^P)^2]^{\frac{1}{2}}. \tag{A55}$$

From (A54) we obtain a lapse rate†

$$\mu = \left[\frac{(n-n_1)(n_2-n)\langle c^2\rangle\langle s^2\rangle}{4\langle -sc'\rangle\langle cs'\rangle}\right]^{\frac{1}{2}} = [(n-n_1)(n_2-n_1)]^{1/2} \tag{A56}$$

within the $\nu_z = \frac{1}{2}$ stop band. Also††

$$n_1 = 0.25 - K/2,$$
$$n_2 = 0.25 + K/2. \tag{A57}$$

† Ref. 4, section IID, especially eq. (2.58), p. 1240.

†† See ref. 4, especially eq. (2.60), p. 1241.

Thus the maximum growth rate is

$$M = K/2 \quad \text{nepers/radian} \tag{A58}$$

or

$$M = \frac{\pi K}{\ln 10} \quad \text{decades/rev}, \tag{A59}$$

and the width of the stop band is

$$\Delta n = n_2 - n_1 = K = \frac{\ln 10}{\pi} M \approx 0.73\, M. \tag{A60}$$

The total growth upon traversing this resonance is

$$G = \int_{n=n_1}^{n_2} \mu d\theta = \frac{\pi^2}{4 \ln 10} \frac{K^2}{|dn/d(\text{rev})|} \text{ decades}. \tag{A61}$$

4. $\nu_r + 2\nu_z = 2(n=0.36)$ Resonance

This resonance has the form of eq. (2) with $m = 2$, indicating that second harmonic azimuthal variations in the field are important for its excitation. In order to allow fully for coupling of free radial oscillations into the axial equation as a first-order perturbation, it is appropriate to develop the B_r component of magnetic field to such an order that eq. (A47) is supplemented by a term proportional to xy. Accordingly, if the B_r component is taken to be given as in eq. (A47) to lowest order by $(1/z)B_r(r,\theta) = (1/r)\xi(r,\theta)$ [where $\xi(r,\theta) = r\,\partial B_z/\partial r = -n(r,\theta)B_z(r,\theta)$ for $z = 0$], one writes

$$\frac{B_r(r,\theta)}{z} \doteq \left.\frac{\xi(r,\theta)}{r}\right|_{r=R} + \left.\frac{\partial\left(\frac{\xi(r,\theta)}{r}\right)}{\partial r}\right|_{r=R} (r-R) \qquad \text{(A62)}$$

or

$$r^2B_r(r,\theta) \doteq R^2(1+2x+\cdots)\left\{\left(-nB_0 + C_2^P\Big|_R \cos 2\theta + S_2^P\Big|_R \sin 2\theta\right) y \right.$$
$$\left. + \left[b''B_0 + R^2\left(\left.\frac{d(C_2^P/r)}{dr}\right|_R \cos 2\theta + \left.\frac{d(S_2^P/r)}{dr}\right|_R \sin 2\theta\right)\right] xy\right\}$$
$$\doteq R^2\left\{\left[-nB_0 + C_2^P\Big|_R \cos 2\theta + S_2^P\Big|_R \sin 2\theta\right] y \right.$$
$$\left. + \left[(b'' - 2n)B_0 + \left.\frac{d(rC_2^P)}{dr}\right|_R \cos 2\theta + \left.\frac{d(rS_2^P)}{dr}\right|_R \sin 2\theta\right] xy\right\}. \qquad \text{(A63)}$$

Insertion of this expression (A63) for r^2B_r into the differential equation for axial motion, $y'' - \frac{r^2B_r}{R^2B_0} = 0$ [cf. (A6)], then yields

$$y'' + \left[n - \frac{1}{B_0}\left(C_2^P\Big|_R \cos 2\theta + S_2^P\Big|_R \sin 2\theta\right)\right] y$$
$$+ \left[2n - b'' - \frac{1}{B_0}\left(\left.\frac{d(rC_2^P)}{dr}\right|_R \cos 2\theta + \left.\frac{d(rS_2^P)}{dr}\right|_R \sin 2\theta\right)\right] xy = 0. \qquad \text{(A64)}$$

For the coupling resonance $2\nu_z + \nu_r = 2$ of present interest we now may ignore the constant term $2n - b''$ in the coefficient of xy in (A64); likewise the alternating component in the coefficient of y does not play a direct role in exciting this resonance, and recognition of this alternating component can be given through use of a ν_y^2 whose value is slightly displaced from n.

Recognizing that the absolute phase of the perturbation is of no importance, the equation for axial motion [eq. (A64)] therefore can be taken to be of the form

$$y'' + (\nu_y^2 - 2\,L\,x \sin 2\theta)\, y = 0, \qquad \text{(A65)}$$

where

$$L = \frac{1}{2B_0}\left\{\left[\left.\frac{d(rC_2^P)}{dr}\right|_R\right]^2 + \left[\left.\frac{d(rS_2^P)}{dr}\right|_R\right]^2\right\}^{1/2}. \qquad \text{(A66)}$$

With the radial oscillations written simply as $x = A_x \sin \nu_x\theta$, eq. (A65) then becomes

$$y'' + \{\nu_y^2 + A_xL[\cos(2+\nu_x)\theta - \cos(2-\nu_x)\theta]\}y = 0. \qquad \text{(A67)}$$

Equation (A67) may be regarded as a Hill equation [especially if we artificially suppose ν_x and $m(=2)$ to be commensurate in some, possibly large, interval]. Noting that eq. (A67) has the form of eq. (2.45) of ref. 4 (taking the lower sign) with

$$a = \nu_y^2 \approx n,$$
$$c = -2A_xL,$$
$$\nu_0 = 2-\nu_x,$$
$$q = 2/\nu_0,$$
$$b = d = 0, \qquad \text{(A68)}$$

we conclude the estimated width of the resonance indicated by the stability boundaries is†

† Ref. 4, especially eq. (2.50), p. 1240.

$$\left|(2\nu_y)^2 - (2-\nu_x)^2\right| = 2\left|LA_x\right| . \tag{A69}$$

If the threshold amplitude is taken to be

$$A_{thr} = 2\,\frac{\left|\nu_y^{\,2} - \left(\frac{2-\nu_x}{2}\right)^2\right|}{|L|} , \tag{A70}$$

then the lapse rate is expected to be†

$$\mu = \left\{\left[\nu_y^{\,2} - \left(\frac{2-\nu_x}{2}\right)^2 + \frac{1}{2}\left|LA_x\right|\right]\left[\left(\frac{2-\nu_x}{2}\right)^2 + \frac{1}{2}\left|LA_x\right| - \nu_y^{\,2}\right]\right\}^{1/2} \Big/ 2\nu_y \tag{A71}$$

or

$$\mu = \frac{|L|}{4\nu_y}\left(A_x^{\,2} - A_{thr}^2\right)^{1/2} \text{ nepers per radian of } \theta . \tag{A72}$$

The maximum growth rate is thus

$$M = \frac{5\pi|L|}{6\ln 10}\left(\frac{A_r}{R}\right) \text{ decades/rev,} \tag{A73}$$

and the total growth is

$$G = \frac{\pi^2}{3(\ln 10)\left|dn/d(\text{rev})\right|}\left(\frac{LA_r}{R}\right)^2 \text{ decades} \tag{A74}$$

with a resonance width of

$$\Delta n = \frac{8|L|}{5}\left(\frac{A_r}{R}\right) = \frac{48\ln 10}{25\pi}\,M \approx 1.4\,M. \tag{A75}$$

† Ref. 4, section IID, especially eq. (2.58), p. 1240.

REFERENCES

1. D. Keefe, G. R. Lambertson, L. J. Laslett, W. A. Perkins, J. M. Peterson, A. M. Sessler, R. W. Allison, Jr., W. W. Chupp, A. U. Luccio, and J. B. Rechen, Phys. Rev. Letters 22 (1969) 558.
2. D. Keefe, W. W. Chupp, A. A. Garren, G. R. Lambertson, L. J. Laslett, A. U. Luccio, W. A. Perkins, J. M. Peterson, J. B. Rechen, and A. M. Sessler, Experiments on Forming, Compressing and Extracting Electron Rings for the Collective Acceleration of Ions (Lawrence Radiation Laboratory Report UCRL-20144, 1970) to be published in Nucl. Instr. and Methods.
3. W. Walkinshaw, A Spiral Ridged Bevatron, A.E.R.E. Report, Harwell, 1956 (unpublished).
4. L. J. Laslett and A. M. Sessler, Rev. Sci. Instr. 32 (1961) 1235.
5. A. A. Garren, D. L. Judd, L. Smith, and H. A. Willax, Nucl. Instr. and Meth. 18, 19, (1962) 525.
6. A. C. Paul, Study of the Regenerative Extractor of the Berkeley 184-Inch Synchrocyclotron, UCRL-18211, April, 1968 (unpublished).
7. W. R. Smythe, Static and Dynamic Electricity, 2nd ed., (McGraw-Hill Book Co., New York, 1950) Sect. 7.14, Eq. (1), p. 275.
8. L. J. Laslett, On an Analytic Solution for Radial Motion When x' Terms Are Included, Lawrence Radiation Laboratory Report ERAN-102, August 1970 (unpublished).

FIGURE CAPTIONS

Fig. 1. The variation of the z component of magnetic field as a function of the azimuthal angle for radii of 18.5 cm and 13 cm at the time of injection.

Fig. 2. Comparison of measured and simulated azimuthally varying fields for a radius of 19 cm at the time of injection.

Fig. 3. The radius of the closed orbit (R), the kinetic energy (T) of the electrons, the magnetic field (B), and the magnetic field index (n) at the location of the closed orbit, as functions of time during the compression of the electron ring for a typical compression cycle.

Fig. 4. Growth rate of axial betatron amplitude for particles injected into a magnetic field that is constant in time, for different values of n (different radii and kinetic energies).

Fig. 5. X-ray signal (due to electrons striking an axial obstacle 1.7 cm from the median plane) as a function of time during a compression cycle in which n at the location of the ring is swept rapidly with the aid of n-shifter circuits; n is determined by calculation and is accurate only to about 0.03.

Fig. 6. X-ray signal showing electron loss on traversal of n = 0.5 resonance.

Fig. 7. Radial and axial betatron amplitudes versus time (number of revolutions) as the n = 0.5 resonance is traversed by a particle in the computer calculation. The initial radial and axial betatron amplitudes are 1.5 cm and 0.1 cm respectively. The upper graph shows how n is varying during this time.

Fig. 8. Radial and axial betatron amplitudes versus time (number of revolutions) for a particle in a constant magnetic field in the middle of the n = 0.5 resonance.

Fig. 9. Radial and axial betatron amplitudes versus time (number of revolutions) for a particle in a constant magnetic field in the middle of the n = 0.2 resonance.

Fig. 10. P_z-z phase-space ellipse as the n = 0.36 resonance is traversed. T refers to the number of revolutions.

Fig. 11. Relation between b" and b"' for vanishing growth rate from eq. (17). The circled points represent a computer check of the analytical formula.

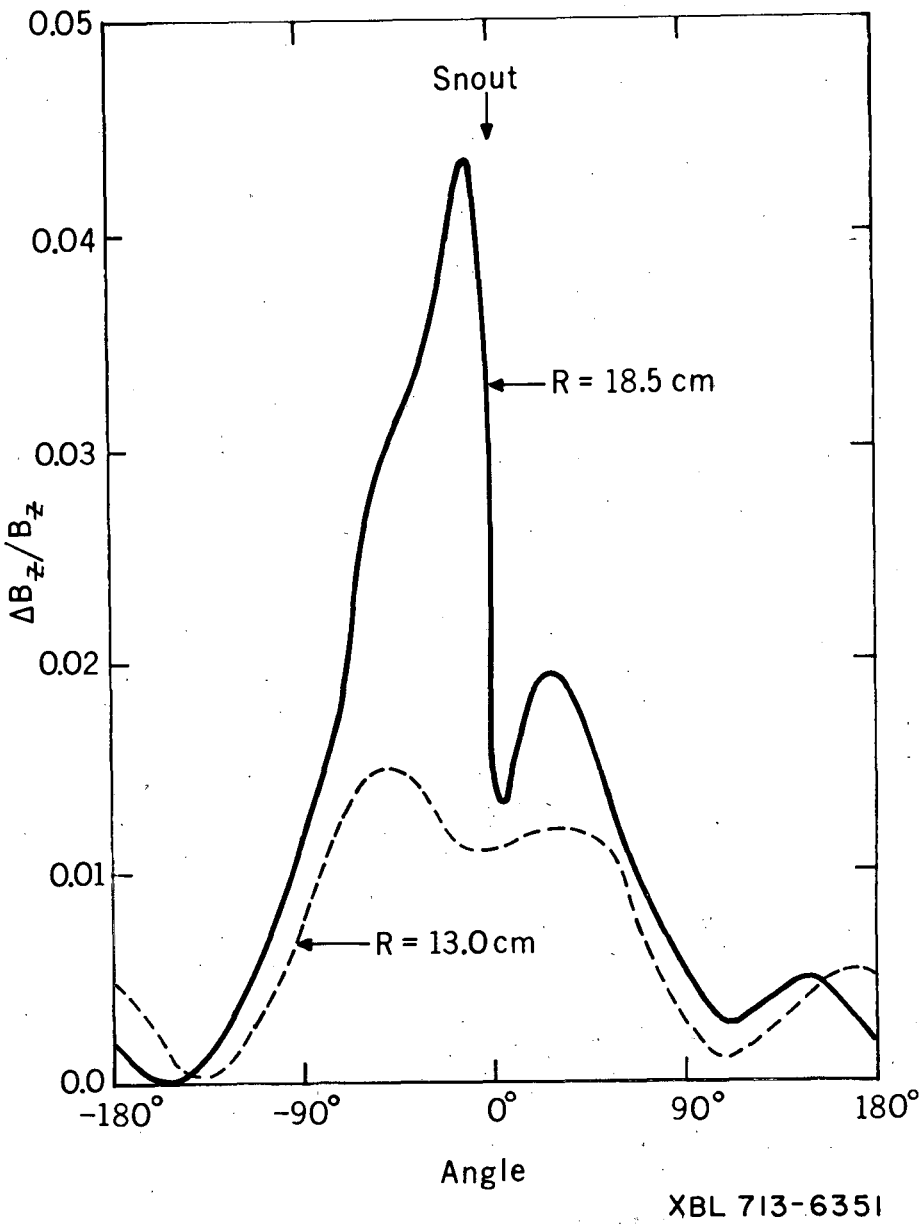

Figure 1

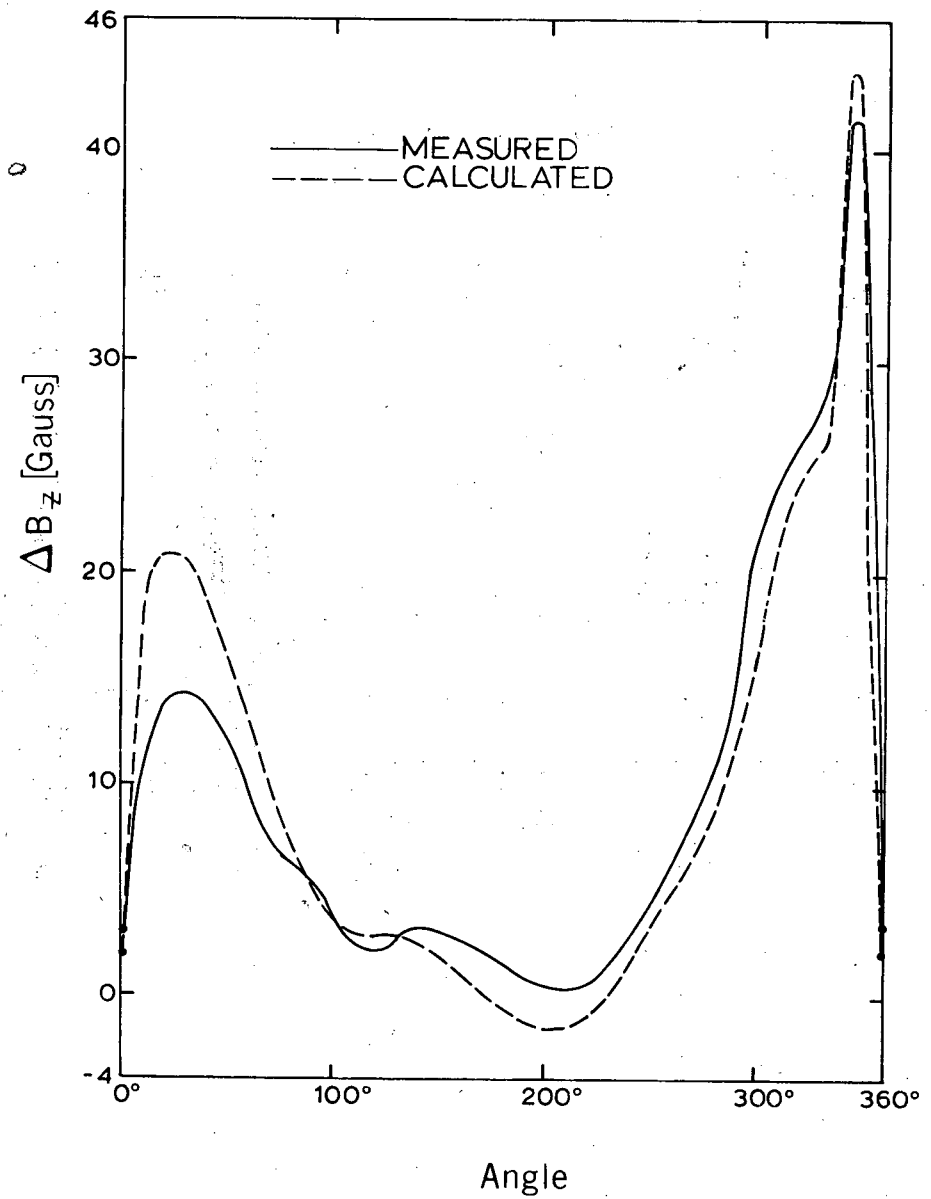

XBL 7010 6261

Figure 2

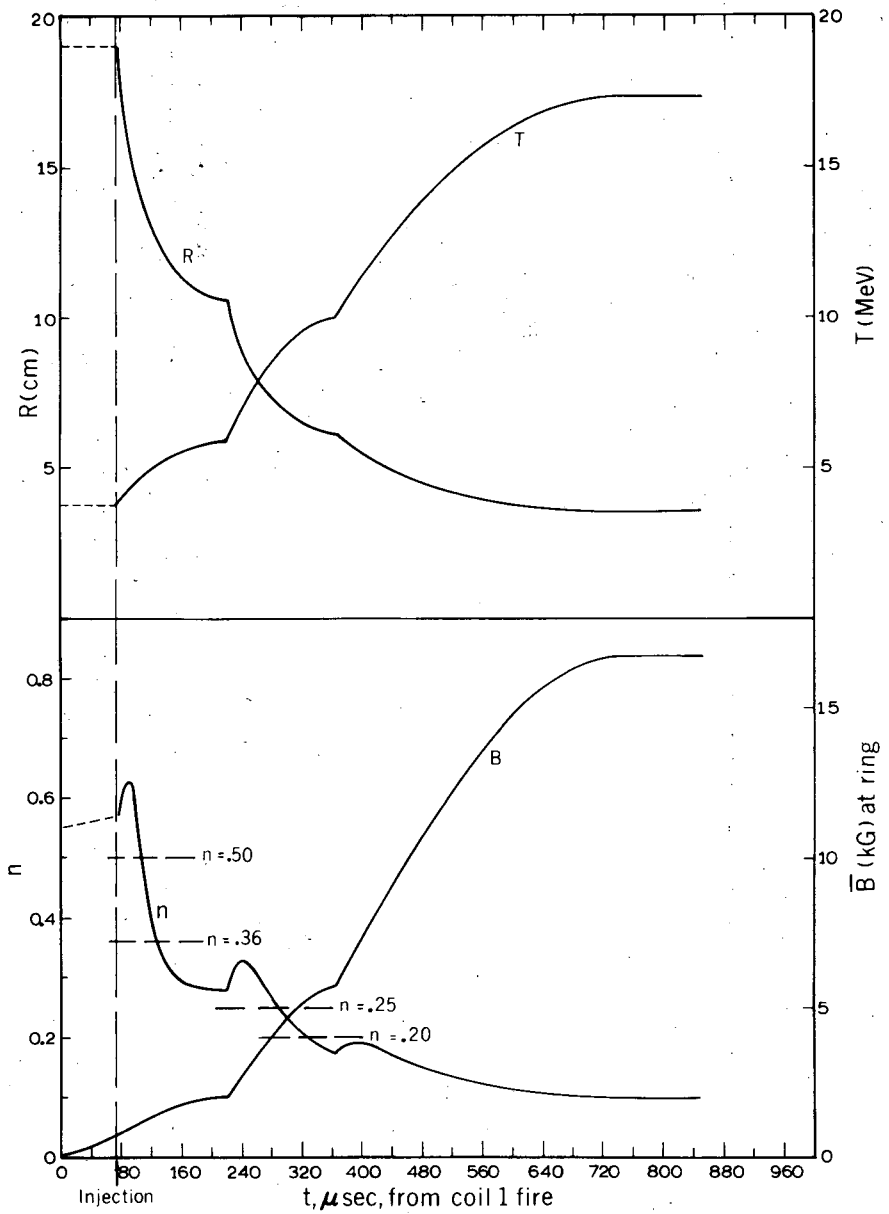

XBL 698 4873

Figure 3

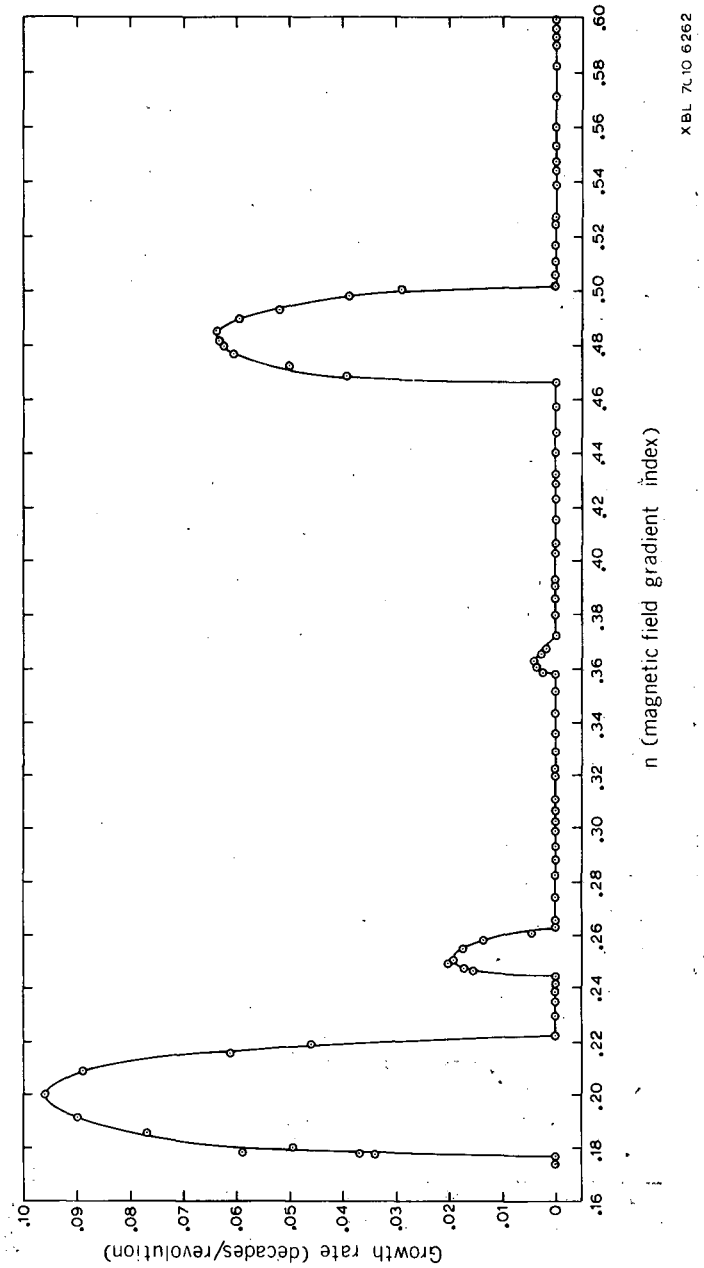

Figure 4

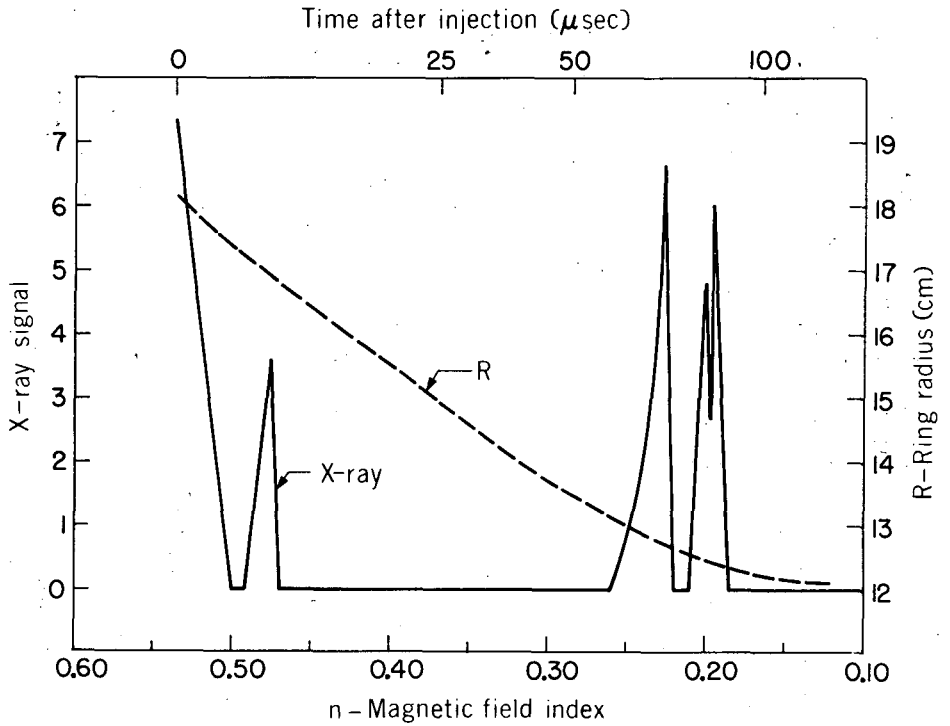

Figure 5

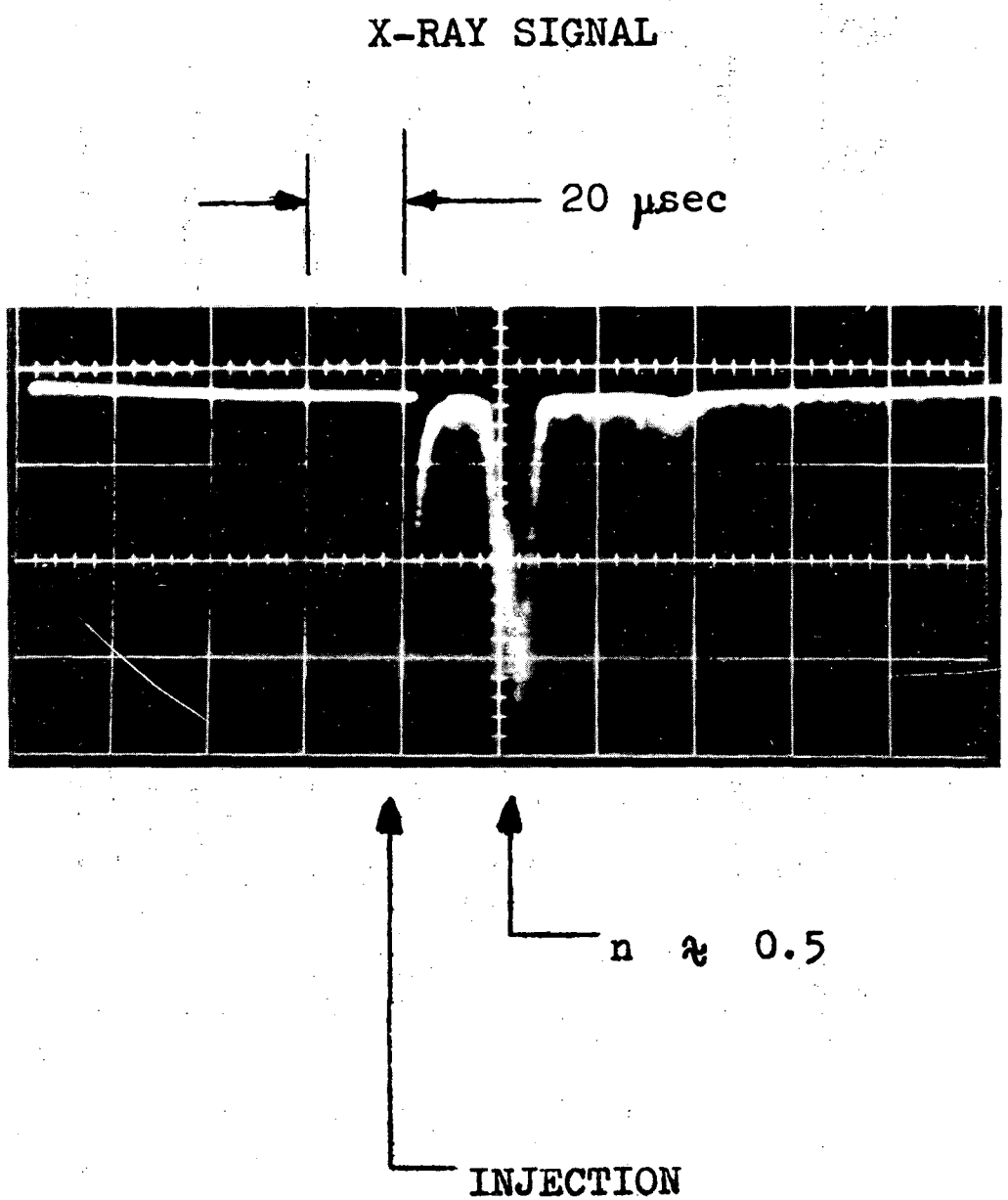

XBB 7011-5339

Figure 6

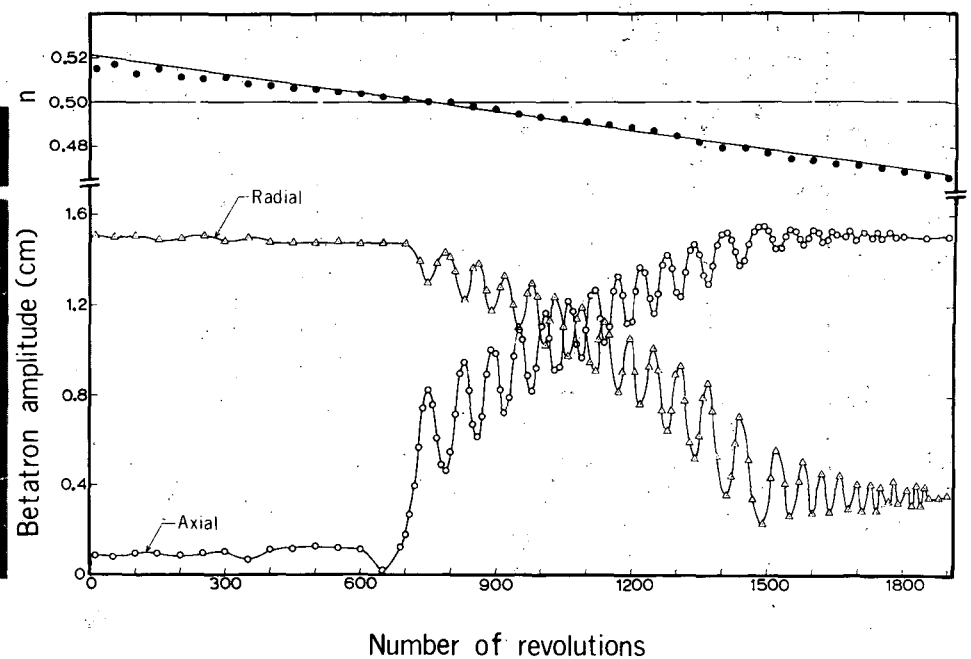

XBL 70106264

Figure 7

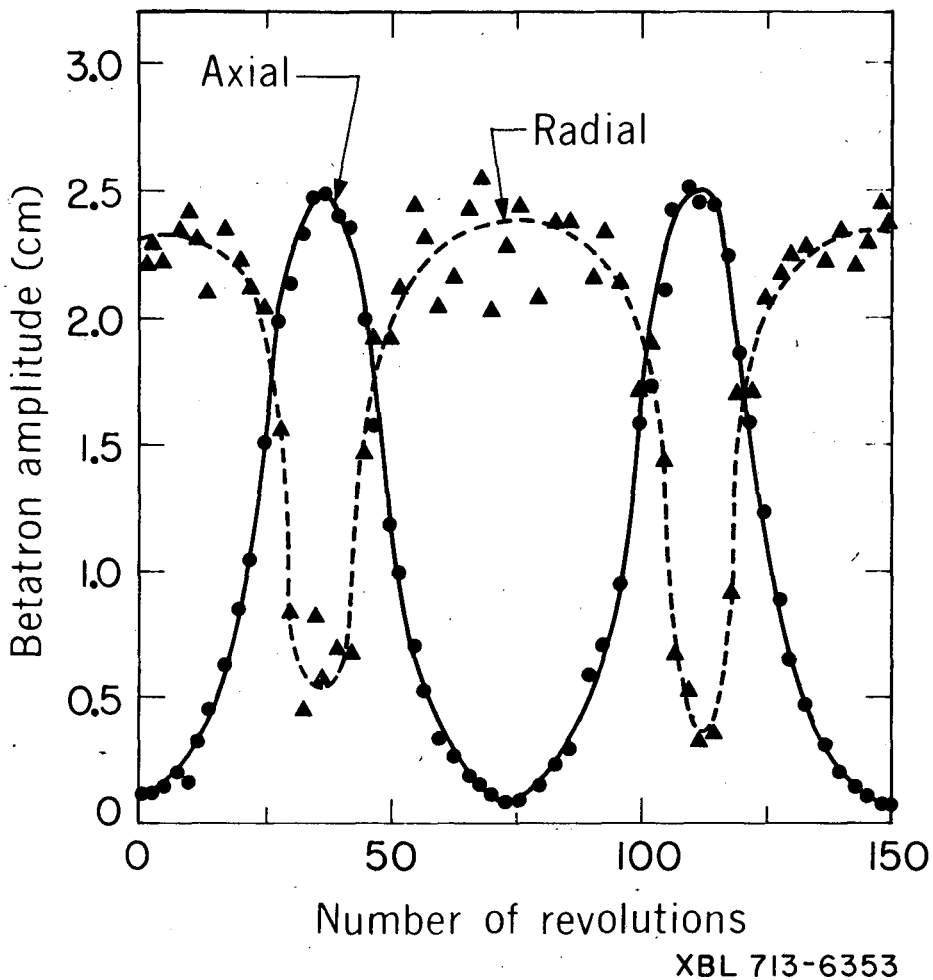

Figure 8

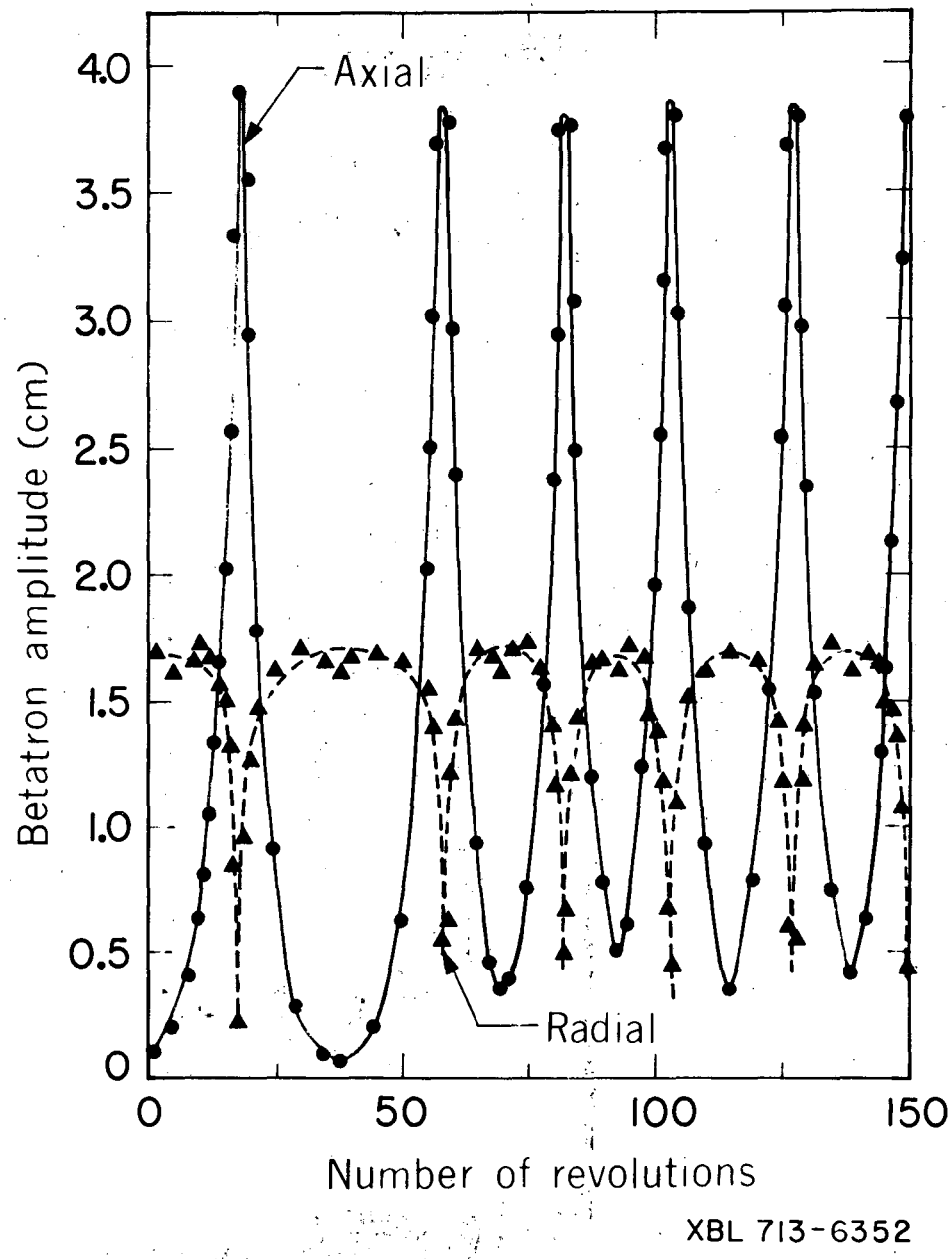

Figure 9

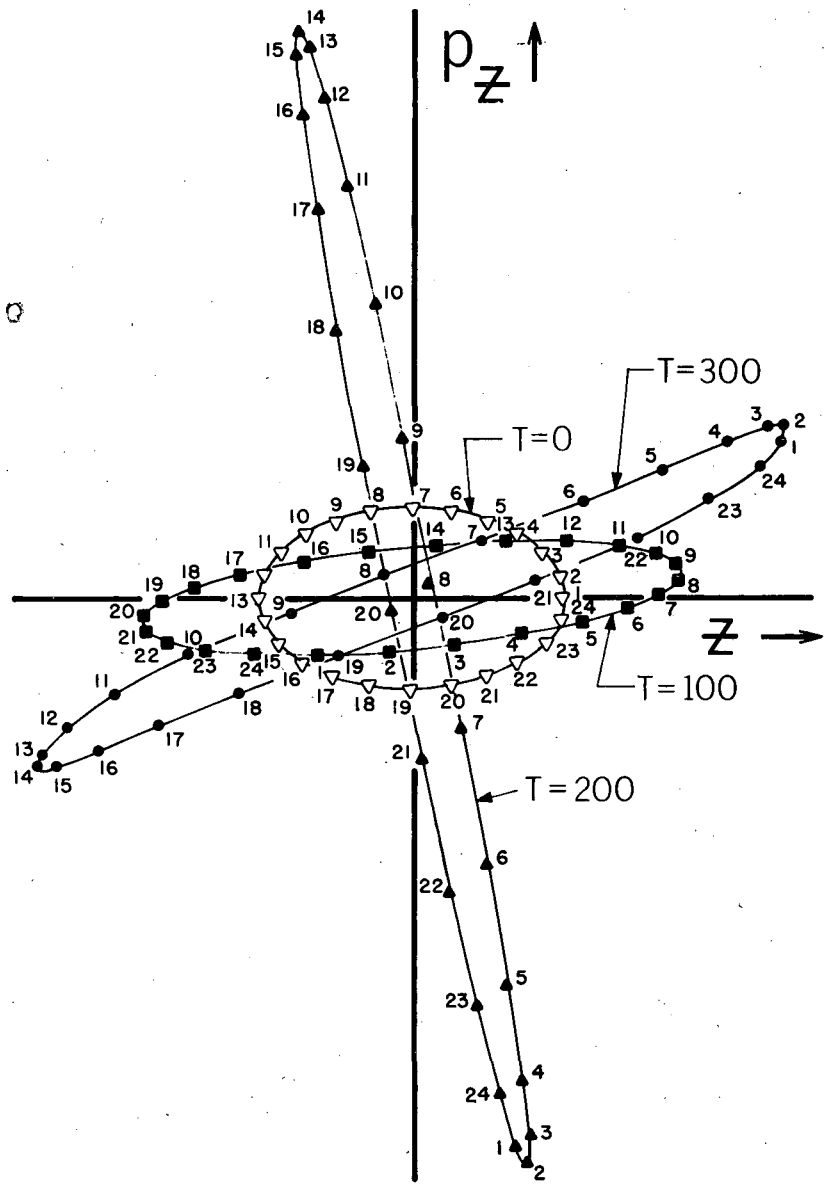

XBL 713-6355

Figure 10

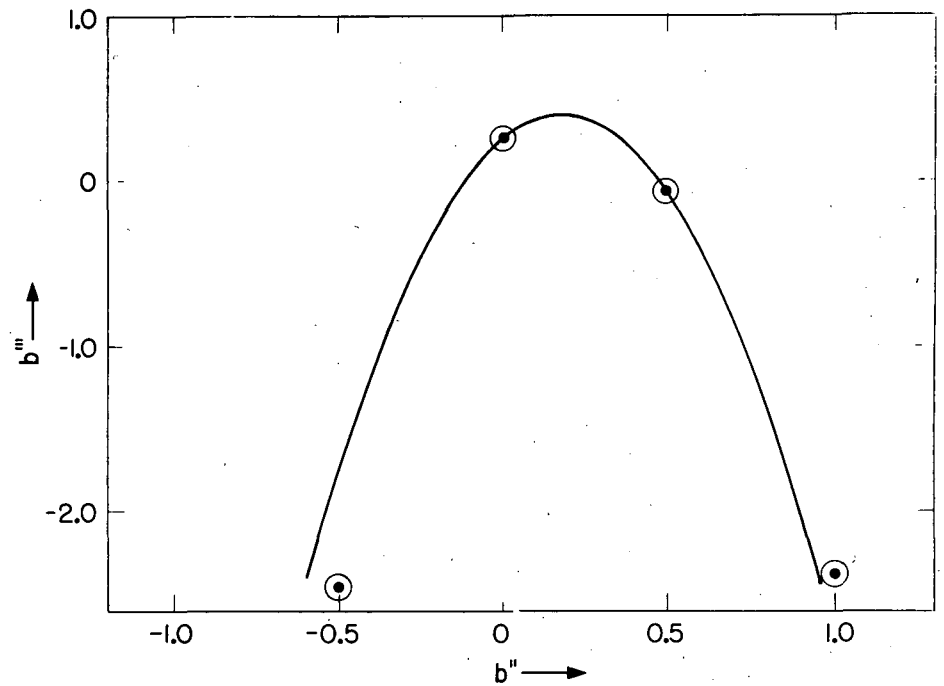

XBL 713-6354

Figure 11

LEGAL NOTICE

This report was prepared as an account of work sponsored by the United States Government. Neither the United States nor the United States Atomic Energy Commission, nor any of their employees, nor any of their contractors, subcontractors, or their employees, makes any warranty, express or implied, or assumes any legal liability or responsibility for the accuracy, completeness or usefulness of any information, apparatus, product or process disclosed, or represents that its use would not infringe privately owned rights.

TECHNICAL INFORMATION DIVISION
LAWRENCE BERKELEY LABORATORY
UNIVERSITY OF CALIFORNIA
BERKELEY, CALIFORNIA 94720